Phys. Status Solidi A **214**, No. 10, 1700372 (2017) / **DOI** 10.1002/pssa.201700372

physica status solidi a
www.pss-a.com
applications and materials science

Electron irradiation of near-UV GaN/InGaN light emitting diodes

In-Hwan Lee[1], Alexander Y. Polyakov[2], N. B. Smirnov[2], I. V. Shchemerov[2], N. M. Shmidt[3], N. A. Tal'nishnih[4], E. I. Shabunina[3], Han-Su Cho[1], Sung-Min Hwang[5], R. A. Zinovyev[2], S. I. Didenko[2], P. B. Lagov[2], and S. J. Pearton*[,6]

[1] Department of Materials Science and Engineering, Korea University, Seoul 02841, Korea
[2] National University of Science and Technology MISiS, 4 Leninsky Ave., Moscow 194017, Russia
[3] Ioffe Physico-Technical Institute, 26 Polytekhnicheskaya Str., St. Petersburg 194021, Russia
[4] Submicron Heterostructures for Microelectronics Research and Engineering Center, St. Petersburg 194021, Russia
[5] Soft-Epi, Inc., Opo-ro 240, Gwangju-si, Gyeonggi-do 464-892, South Korea
[6] Department of Materials Science and Engineering, University of Florida, Gainesville, FL 32611, USA

Received 13 June 2017, revised 13 June 2017, accepted 26 June 2017
Published online 21 July 2017

Keywords defects, electroluminescence, electron irradiation, GaN, LED

* Corresponding author: email spear@mse.ufl.edu, Phone: +1-352-846-1086, Fax: +1-352-846-1182

Irradiation with 6 MeV electrons of near-UV (peak wavelength 385–390 nm) multi-quantum-well (MQW) GaN/InGaN light emitting diodes (LEDs) causes an increase in density of deep electron traps near E_c−0.8 and E_c−1 eV, and correlates to a 90% decrease of electroluminescence (EL) efficiency after a fluence of $1.1 \times 10^{16}\,cm^{-2}$. The likely origin of the EL efficiency decrease is this increase in concentration of the E_c −0.8 eV and E_c −1 eV traps.

1 Introduction Light emitting diodes (LEDs) based on multiple quantum wells (MQWs) of AlGaN/GaN or AlGaN/InAlGaN and operating in the near-UV (NUV) spectral region of 320–400 nm (UVA class LEDs) are of interest for applications in 3D printing, UV curing, UV lithography, sensing, medicine and biology, and security [1–3]. The performance of this class of LEDs has improved greatly, leading to their widespread use [1, 2]. The main problems limiting performance in these LEDs are the poor confinement of charge carriers in relatively shallow GaN/InGaN QWs for wavelengths close to 400 nm, generally higher dislocation densities compared to blue LEDs and lower light extraction efficiency caused mainly by self-absorption in the top p-GaN contact layer [1–3]. Little is known about the deep electron and hole traps present in NUV LEDs, and the effects on their performance of irradiation with high energy particles. It would be clearly beneficial to better understand the type and nature of deep traps in NUV LEDs. Changes induced by electrical stress of LED-like 400 nm laser diodes have been reported [4, 5]. It was found that electrical stress gave rise to increased leakage of the diodes at low forward voltage. This increased leakage correlated with the decrease of EL efficiency [4]. The degradation of EL efficiency upon electrical stress correlated with the emergence of a broad defect band in electron traps spectra [5]. The deep trap spectra of NUV LEDs are dominated by electron traps with levels near E_c −0.8 eV and hole traps in the QWs with levels near E_v +0.75 eV [6]. One of the best ways to controllably alter the deep trap concentration and to assess the impact of various centers on performance of semiconductor devices is to study the influence of bombardment with high energy particles on device performance. Though radiation effects in LEDs have been studied in a number of publications [7–12], no detailed studies on deep trap spectra in NUV LEDs have been published. In this letter, we present results of a study on the influence of 6 MeV electron irradiation on NUV LEDs.

2 Experimental The MQW GaN/InGaN structures consisted of a thin low-temperature GaN nucleation layer, 4 μm of unintentionally doped nGaN, 2 μm of n^+GaN (donor concentration $\sim 5 \times 10^{18}\,cm^{-3}$, a strain relieving InGaN/AlGaN superlattice (100 nm), 6 GaN/InGaN QWs (nominal In composition in the QWs ~ 5%, undoped QW width 2.5 nm, the GaN barrier width 10 nm), p-AlGaN electron blocking layer (EBL; Al composition 15%, thickness of 25 nm, doping $10^{17}\,cm^{-3}$), and p-GaN top contact layer (room temperature hole concentration of $\sim 3\times 10^{17}\,cm^{-3}$ from Hall measurements, thickness 100 nm). The structures were processed into 1.1 mm × 1.1 mm mesas by dry etching, with the ohmic contact to n^{+}GaN made by Ti/Al deposition and annealing, and the Ohmic contact to p-GaN made by deposition of a thin layer of indium tin oxide (ITO) with Ag electrodes on top. The diodes were characterized before and after electron irradiation with current–voltage (*I–V*) measurements, capacitance–voltage (*C–V*) profiling, admittance spectra (AS) [13], deep level transient spectroscopy with electrical (DLTS), and optical (ODLTS) [14] injection performed in the temperature range 90–400 K.

Electron irradiation was performed in a linear electron accelerator, with electron energy 6 MeV, electron fluences of $10^{11}\,cm^{-2}\,s^{-1}$, with fluencies 10^{15}, 3×10^{15}, 6×10^{15}, and $1.1\times 10^{16}\,cm^{-2}$ [13–17]. The LEDs had state-of-the-art electrical and optical characteristics. The reverse current was $\sim 10^{-8}$ A at −3 V, the ideality factor in the forward direction was 2.3, the series resistance at forward voltage >3 V was ~0.7 Ω and the forward current in the exponential region increased with an activation energy of 0.45 eV.

3 Results and discussion Figure 1 shows a typical 300 K *I–V* before irradiation. After irradiation, neither the reverse leakage current nor the ideality factor changed significantly, even for the highest electron fluence of $1.1\times 10^{16}\,cm^{-2}$ (Fig. 1(a)). However, we did observe a gradual increase of the diode series resistance at high forward bias with increasing fluence, as shown in Fig. 1(b).

The concentration profile of the LEDs before irradiation indicated the edge of the space charge region (SCR) at 0 V was located below the lowermost InGaN QW (Fig. 2(a)). To sweep the SCR through the lowest QW, the voltage had to be increased to 2 V. The corresponding width of the MQW region, estimated from the concentration profile in Fig. 2, was 80 nm, in good agreement with the designed value. The profiles measured under illumination with high-power LEDs with peak photon energies between 1.3 and 3.4 eV were not significantly different from the dark profile, indicating there was a low density of deep traps in the bandgap. After irradiation with the highest 6 MeV electron fluence of $1.1\times 10^{16}\,cm^{-2}$, the dark concentration profile did not change, but there appeared significant photocapacitance with subbandgap illumination. The profile taken under illumination with 2 eV photons is shown for the irradiated sample in Fig. 2. The spectrum showed a clear optical threshold near a photon energy of 1.3 eV and a near plateau between 1.5 and 2 eV. The concentration of the center responsible for this photocapacitance was calculated as the difference between the *C–V* concentration at 2 eV and in the dark [18–20] and it was $\sim 10^{16}\,cm^{-3}$. From the concentration profile under illumination, the centers are located in the GaN barrier of the QW. These are often observed in photocapacitance profiles of n-GaN and attributed to carbon interstitials [21].

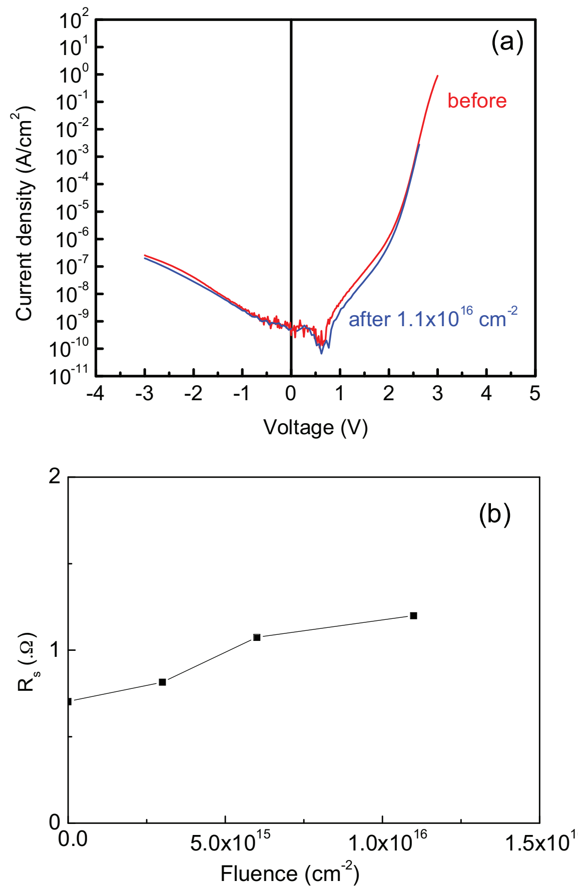

Figure 1 (a) 300 K *I–V* characteristics of the LED before (red line) and after (blue line) irradiation with $1.1\times 10^{16}\,cm^{-2}$ 6 MeV electrons; (b) series resistance at high forward voltage as a result of electron irradiation.

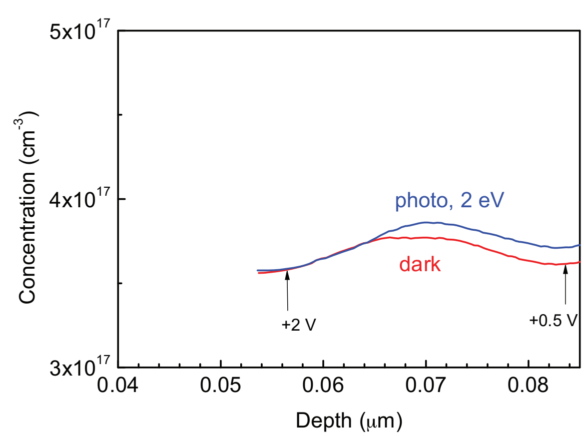

Figure 2 Concentration profiles calculated from 300 K *C–V* characteristics in the dark before irradiation and after $1.1\times 10^{16}\,cm^{-2}$ 6 MeV electron irradiation (red line, profiles are the same) and the profile after irradiation (blue line) measured under illumination with 2 eV LED.

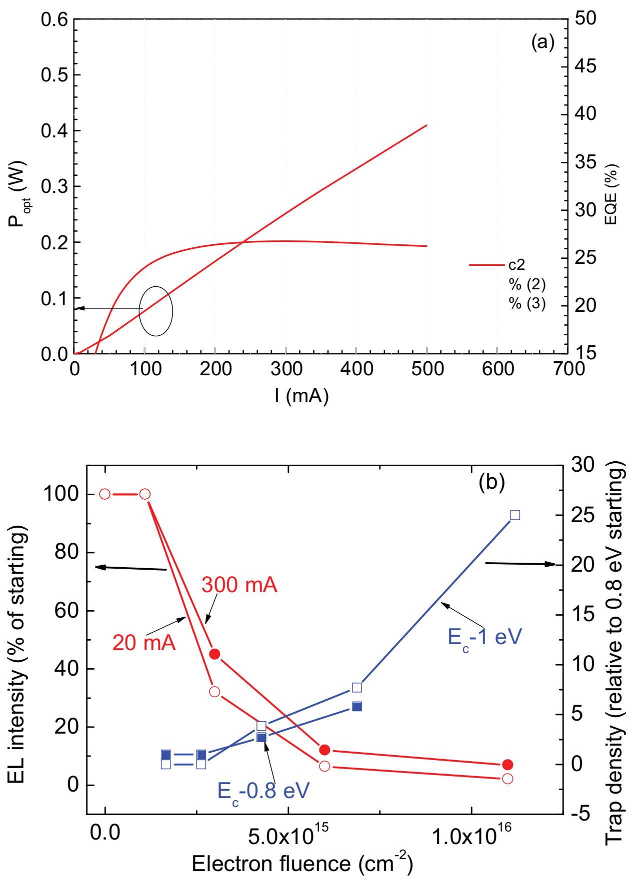

Figure 3 (a) EL power output (left axis) and EQE (right axis) of the LEDs before irradiation; (b) changes with electron fluence of the EL power (red curves, left axis) at driving currents 20 mA (open circles) and 300 mA (solid circles), the data normalized to pre-irradiation values; blue lines (right axis) show the dependence of the $E_c - 0.8$ eV (solid squares) and $E_c - 1$ eV (open squares) electron traps DLTS signal on the electron fluence; the data normalized to the starting signal of the $E_c - 0.8$ eV trap.

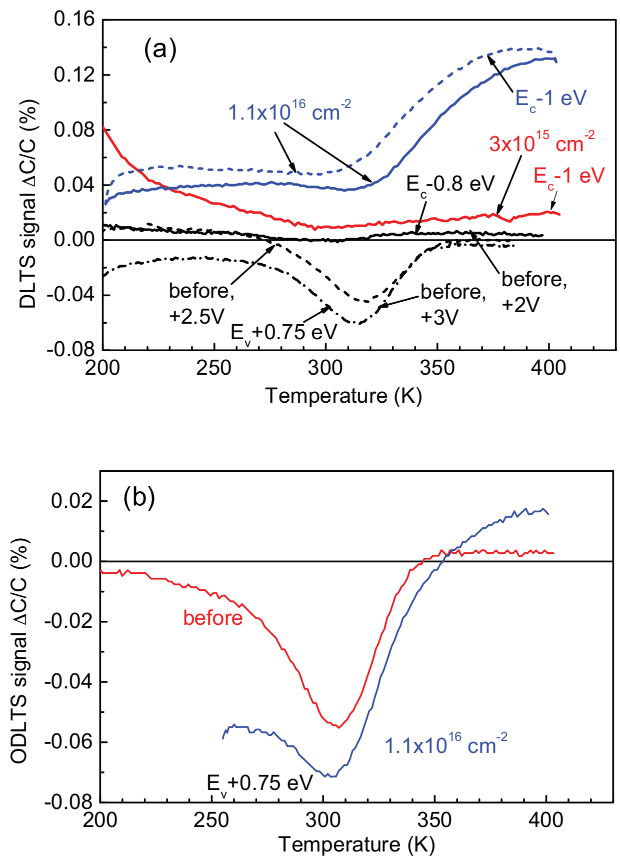

Figure 4 (a) DLTS spectra of LEDs before irradiation (black lines) obtained at +0.5 V bias, forward bias pulses of +2 V (solid line), +2.5 V (dashed line), +3 V (dash-dotted line), time windows 700 ms/7000 ms; red line-the spectrum measured after irradiation with 3×10^{15} cm^{-2} electrons, forward bias +2 V, time windows 700 ms/7000 ms; blue lines-spectra measured after irradiation at 1.1×10^{16} cm^{-2}, time windows 700 ms/7000 ms (solid line) and 1750 ms/17500 ms (dashed line); (b) ODLTS spectra of LED before (red line) and after irradiation with 1.1×10^{16} cm^{-2} electrons (blue line); bias +0.5 V, excitation with photon energy 3.4 eV, time windows 1250 ms/12500 ms.

The EL spectrum of the LEDs consisted of one main line peaked at photon energy 3.2 eV. Figure 3(a) shows the output power of the LEDs (left ordinate axis) on the driving forward current and the calculated dependence of the external quantum efficiency (EQE) of the LEDs on current. The output power was 180 mW at 500 mA. The EQE was close to 25% and showed very small droop with increasing current. Electron irradiation with the fluence of 1×10^{15} cm^{-2} did not change the EL characteristics. For higher fluences, the output power gradually decreased, with a stronger effect for lower driving current (in Fig. 3(b) we show the changes of EL power normalized to the starting value for drive currents of 20 and 300 mA).

DLTS spectra of the LEDs (Fig. 4(a)) before irradiation showed the presence of electron traps near $E_c - 0.8$ eV and hole traps near $E_v + 0.75$ eV. These are attributed to defects in the InGaN QWs [6]. The electron traps are similar to the $E_c - 1$ eV traps commonly found in n-GaN and are likely related to nitrogen interstitial acceptors N_I [22–24]. The $E_v + 0.75$ eV hole traps have been attributed to the same defects that give rise to the main hole traps in n-GaN near $E_v + 0.9$ eV responsible for the yellow luminescence band [24]. The magnitude of the DLTS peak due to the $E_v + 0.75$ eV hole traps depended strongly on the density of injected holes, i.e., on applied forward voltage. The DLTS peak magnitude increased rapidly as the forward bias pulse amplitude increased from +2 to +2.5 V. For higher bias pulses, the peak amplitude saturated. The $E_v + 0.75$ eV hole traps also dominated the ODLTS spectra obtained with excitation wavelengths generating electron-hole pairs only in the InGaN QWs (photon energy 3.2 eV) or both in the GaN barriers and in the InGaN QWs (photons with energy 3.4 eV). The trap signature and the peak amplitude were similar in both cases if the output power of the excitation LED in ODLTS was adjusted to ensure saturation of the peak amplitude.

Figure 4(b) shows an ODLTS spectrum taken before irradiation with excitation from 3.4 eV LEDs. The spectra are for temperatures higher than 200 K – at lower temperatures the capacitance decreased strongly due to freeze-out of Mg acceptors in p-GaN and reliable DLTS measurements were not practicable [6, 17, 18]. The quiescent bias used for DLTS and ODLTS measurements in Fig. 4 was +0.5 V to place the SCR edge close to the MQW region. Since the peaks of the electron and hole traps in DLTS overlap and interfere, the spectra after irradiation were taken with forward bias pulses of +2 V to minimize the impact of the hole trap peak on the amplitude of the electron trap peak. The changes in the concentration of the hole traps were measured by the amplitudes of the hole trap peak in ODLTS. The concentration of the E_v +0.75 eV hole traps did not change significantly even after irradiation with the highest fluence. By contrast, the electron traps in the DLTS spectra were not changed after irradiation with 1×10^{15} cm^{-2} of 6 MeV electrons. For higher fluences, we observed a broad feature that could be deconvoluted into peaks corresponding to the Ec −0.8 eV and E_c −1 eV electron traps instead of the E_c −0.8 eV peak.

For the highest fluence of 1.1×10^{16} cm^{-2}, the E_c −1 eV peak became dominant, as shown in Fig. 4(a). In Fig 3(b), we display the electron fluence dependence of the amplitudes of respective peaks normalized to the starting amplitude of the E_c −0.8 E_v peak. The concentrations of both species increased rapidly after irradiation.

What is the origin of the decrease of the EL efficiency after electron irradiation of our NUV LEDs? The most likely explanation is the increase in concentration of the E_c −0.8 eV and E_c −1 eV electron traps. The change in the density of these traps correlates with the decrease of EL power. The E_c −1 eV traps that dominate after irradiation with high doses of electrons have signatures similar to those of the E_c −1 eV traps shown to be major lifetime killers in electron irradiated n-GaN [14]. Since the E_c −0.8 eV traps are believed to be due to similar defects (Ni-) located in InGaN QWs [6] it is logical to also associate them with efficient lifetime killers.

Other deep traps detected in our NUV LEDs do not seem to be important for EL degradation. The density of the E_v +0.75 eV hole traps does not change significantly after irradiation. Moreover, if these traps are similar to the major E_v +0.9 eV hole traps in n-GaN [6], one would not expect them to effectively influence the recombination lifetime and this was demonstrated experimentally [20, 25]. The traps with optical threshold near 1.3 eV whose concentration increased after irradiation are similar to the centers often observed in n-GaN and attributed to carbon interstitials [21–24]. These centers are not likely to be major lifetime killers [20, 25]. However, part of the degradation of the EL power after irradiation could come from the diode series resistance.

Acknowledgements The work at NUST MISiS was supported by the Ministry of Education and Science of the Russian Federation in the framework of Increase Competitiveness Program of NUST (MISiS) (K2-2014-055). The work at Korea University was supported by National Research Foundation of Korea Ministry of Science, ICT & Future Planning (2017R1A2B3006141). UF was supported by DTRA HDTRA1-17-1-0011.

References

[1] M. Kneissl, in: A Brief Review of III-Nitride UV Emitter Technologies and Their Applications, in III-Nitride Ultraviolet Emitters, edited by M. Kneissl and J. Rass (Springer International Publishing, Switzerland, 2016), chap. 1.

[2] Y. Muramoto, M. Kimura, and S. Nouda, Semicond. Sci. Technol. **29**, 084004 (2014).

[3] C. Jia, T. Yu, X. Feng, K. Wang, and G. Zhang, Superlattices Microstruct. **97**, 417 (2016).

[4] M. Meneghini, N. Trivellin, K. Orita, S. Takigawa, T. Tanaka, D. Ueda, G. Meneghesso, and E. Zanoni, Appl. Phys. Lett. **97**, 263501 (2010).

[5] M. Meneghini, C. de Santi, N. Trivellin, K. Orita, S. Takigawa, T. Tanaka, D. Ueda, G. Meneghesso, and E. Zanoni, Appl. Phys. Lett. **99**, 093506 (2011).

[6] I.-H. Lee, A. Y. Polyakov, N. B. Smirnov, R. A. Zinovyev, K.-B. Bae, T.-H. Chung, S.-M. Hwang, J. H. Baek, and S. J. Pearton, Appl. Phys. Lett. **110**, 192107 (2017).

[7] S. J. Pearton, F. Ren, E. Patrick, M. E. Law, and A. Y. Polyakov, ECS J. Solid State Sci. Technol. **5**, Q35 (2016).

[8] S. M. Khanna, D. Estan, A. Houdayer, H. C. Liu, and R. Dudek, IEEE Trans. Nucl. Sci. **51**, 3585 (2004).

[9] F. Gaudreau, C. Carlone, A. Houdayer, and S. M. Khanna, IEEE Trans. Nucl. Sci. **48**, 1778 (2001).

[10] R. Khanna, S. Y. Han, S. J. Pearton, D. Schoenfeld, W. V. Schoenfeld, and F. Ren, Appl. Phys. Lett. **87**, 212107 (2005).

[11] B.-J. Kim, Y.-H. Hwang, S. Ahn, F. Ren, S. J. Pearton, J. Kim, and T. S. Jang, J. Vac. Sci. Technol. B **33**, 051215 (2015).

[12] R. Khanna, K. K. Allums, C. R. Abernathy, S. J. Pearton, J. Kim, F. Ren, R. Dwivedi, T. N. Fogarty, and R. Wilkinsd, Appl. Phys. Lett. **85**, 3131 (2004).

[13] L. Pautrat, B. Katircioglu, N. Magnea, D. Bensahel, J. C. Pfister, and L. Revoil, Solid-State Electron. **23**, 1159 (1980).

[14] G. M. Martin, A. Mitonneau, D. Pons, A. Mircea, and D. W. Woodard, J. Phys. C **13**, 3855 (1980).

[15] A. Y. Polyakov, N. B. Smirnov, I.-H. Lee, and S. J. Pearton, J. Vac. Sci. Technol. B **33**, 061203 (2015).

[16] I.-H. Lee, A. Y. Polyakov, N. B. Smirnov, A. S. Usikov, H. Helava, N. Yu. Makarov, and S. J. Pearton, J. Appl. Phys. **115**, 223702 (2014).

[17] I.-H. Lee, H.-S. Cho, K. B. Bae, A. Y. Polyakov, N. B. Smirnov, R. A. Zinovyev, J. H. Baek, T.-H. Chung, I. V. Shchemerov, E. S. Kondratyev, and S. J. Pearton, J. Appl. Phys. **121**, 045108 (2017).

[18] A. Y. Polyakov, N. B. Smirnov, E. B. Yakimov, H.-S. Cho, J. H. Baek, A. V. Turutin, I. V. Shemerov, E. S. Kondratyev, and I.-H. Lee, ECS Solid State Sci. Technol. **5**, Q274 (2016).

[19] I.-H. Lee, A. Y. Polyakov, E. B. Yakimov, N. B. Smirnov, I. V. Shchemerov, S. A. Tarelkin, S. I. Didenko, K. I. Tapero, R. A. Zinovyev, and S. J. Pearton, Appl. Phys. Lett. **110**, 112102 (2017).

[20] I.-H. Lee, A. Y. Polyakov, N. B. Smirnov, E. B. Yakimov, S. A. Tarelkin, A. V. Turutin, I. V. Shemerov, and S. J. Pearton, J. Appl. Phys. **119**, 205109 (2016).

[21] Z. Zhang, A. R. Arehart, E. Cinkilic, J. Chen, E. X. Zhang, D. M. Fleetwood, R. D. Schrimpf, J. S. Speck, and S. A. Ringel, Appl. Phys. Lett. **103**, 042102 (2013).
[22] A. Sasikumar, A. R. Arehart, G. D. Via, B. Winningham, B. Poling, E. Heller, and S. A. Ringel, Microelectron. Reliab. **55**, 2258 (2015).
[23] J. L. Lyons, A. Janotti, and C. G. Van de Walle, Phys. Rev. B **89**, 035204 (2014).
[24] A. Y. Polyakov and I.-H. Lee, Mat. Sci. Eng. R **94**, 1 (2015).
[25] I.-H. Lee, A. Y. Polyakov, N. B. Smirnov, E. B. Yakimov, S. A. Tarelkin, A. V. Turutin, I. V. Shemerov, and S. J. Pearton, Appl. Phys. Express **9**, 061002 (2016).